

A Model of the Proton (Revised)

R Wayte

29 Audley Way, Ascot, Berkshire SL5 8EE, England, UK

email: rwayte@googlemail.com

Submitted to vixra.org 18 October 2019

Abstract. A composite model of the proton is developed which satisfies general empirical features. A Yukawa-type potential is incorporated into Einstein's equations of general relativity to predict a hadronic force constant 76.6 times stronger than the fine structure constant. Proton mass is expressed in terms of muonic mass building-blocks. Analysis of the magnetic moment allows substructure modelling wherein creation of component parts is described in terms of action-integrals. The gluon colour field is related to hadronic force and proton energy. Uniqueness of electromagnetic charge is attributed to a governing action principle. A neutron model has been proposed comprising a proton orbited by a heavy-electron. Compatibility with the quarks of the Standard Model has been established regarding interactions between particles.

PACS: 12.39.Pn, 12.60.Rc, 14.20.Dh

1. Introduction

Proton design is much more complicated than the electron model (Wayte, Paper 1) or muon model (Wayte, Paper 2). Although proton charge is exactly equal and opposite to the electronic charge, the proton magnetic moment is nearly 3 times the expected value. In addition, the proton has a strong but short-range hadronic/nuclear force field which does not interact with leptons or electric fields. During high-energy collisions, the proton appears to consist of 3 smaller particles, but the amount of spin held by these individuals is still debatable. Established QCD theory has offered explanations for most aspects of proton behaviour; see textbooks such as Perkins (2000), Martin & Shaw (1997), Fraunfelder & Henley (1991). However, experiments with spin-directed protons strain this theory (Krisch, 1992). Some experiments on proton electric/magnetic form factors indicate a quark-like core plus mesonic cloud field, (Iachello, 2004). Other experiments on electron-nucleon scattering, to determine radii of a proton and neutron, have been reviewed by Sick (2005).

Our proton model is compatible with previous electron and muon models, independent of QCD theory. The paper is divided into sections:

- (2): hadronic potential of an inherent sizeable quantum field.
- (3): Einstein's equations describe a Yukawa-type field with hadronic force constant.
- (4): hard core repulsion attributed to rotation of the proton core modulating the field.
- (5): proton magnetic moment analysed in terms of substructures.
- (6): proton mass expressed in terms of muon mass.
- (7): creation of proton sub-structures in terms of action integrals.
- (8): gluon field holding component structures together.
- (9): uniqueness of electromagnetic charge.
- (10): neutron model consisting of a proton plus heavy-electron.
- (11): compatibility with QCD theory for interactions between particles.

Proton features are *tangible* and revealed as electromagnetic charge, nebulous hadronic force-field, hard-core repulsion, internal gluon field, mass relative to leptons, real spin angular momentum, magnetic moment and substructure. Essential properties are the conservation of energy and momentum, and compatibility with relativity theory.

Postulations of negative energy, time reversal, extra dimensions, point quarks, abstract spin, Higgs bosons, and non-conservation of energy have not been considered realistic.

All fundamental physical constants and particle properties have been taken from the latest 2019 measured values given in <http://physics.nist.gov/constants> and <http://pdg.lbl.gov>.

2. The hadronic potential

The necessity for this derivation of potential is clear. Signell (1980) stated that his preferred potential would have to be realistic and match the NN data. Other investigators complain that the dozens of variables in a complex theory is a sign that a better way must exist. Accordingly, the phenomenological profile predicted by Stoks et al. (1994) which fits quality data will be taken as a realistic guide towards a better potential.

In our proton model there are 9 pearls of mass ($m_\ell = m_p/9$) constituting the proton, which carry the exterior nebulous nuclear field charge-quanta. (The pearls actually form 3 trineons analogous to but not equal to quarks). The Klein-Gordon wave equation will be taken as the basis of our own inter-nucleon potential as described by Yukawa:

$$\frac{1}{c^2} \frac{\partial^2 \Psi}{\partial t^2} = \nabla^2 \Psi - \left(\frac{m_\ell c}{\hbar} \right)^2 \Psi = \nabla^2 \Psi - \left(\frac{1}{r_\ell} \right)^2 \Psi \quad , \quad (2.1)$$

where ($r_\ell = \hbar/m_\ell c = 1.89278$ fm) is the natural internal pearl Compton radius, rather than the foreign pionic radius propounded in QCD theory. If we assume that this wave amplitude Ψ is proportional to potential $V(r)$, then for a static potential the solution of (2.1) in a spherically symmetric form is:

$$V(r) = -a_Y \frac{\exp-(r/r_\ell)}{r} \quad , \quad (2.2)$$

where (a_Y) represents hadronic/nuclear charge. This exterior field carried by the pearls is copious and may be regarded as a residual or concomitant part of the interior strong interaction force carried by pearls between the constituent components in the proton core, see Section 8. Pearls herein are roughly equivalent to gluons in QCD theory.

Potential $V(r)$ is attractive and applies for nucleon-nucleon ranges beyond 1.9fm, but experiments imply a repulsive hard core potential below 0.8fm. Therefore, several useful potential models have been developed over the years wherein meson exchange was

invoked for the attractive part while the repulsive core was phenomenological. Comparisons of these suggested potentials have been illustrated by Signell (1980) and Bugg (1981). More recently, three potential models have been endorsed by Stoks et al. (1994) for fitting very well to the latest data. They and others saw great value in deriving a potential profile which could usefully fit data numerically, even without understanding all the physics involved.

We shall now derive a relativistic expression for the natural field of a quiescent nucleon (neglecting spin), as would be experienced by a theoretical *infinitesimal* test particle. Then this will be extended to describe the real NN-interaction field actually experienced by a true-size nebulous nucleon in an energetic collision.

3. Application of Einstein's equations

For Einstein's equations to interpret the hadronic force in a way compatible with the electromagnetic force, the metric tensor component might be expected to have the simple form:

$$\gamma = \left\{ 1 + \frac{a_Y V(r)}{m_p c^2} \right\}, \quad (3.1)$$

where m_p is the proton mass and $V(r)$ is given by (2.2), (see Paper 1, Section 1.8, and Wayte 1983). However, this expression would lead to regions of *negative* field energy, but a realistic form compatible with Poisson's Equation for a proton field is:

$$\gamma = \left\{ 1 - 2 \left(\frac{a_Y^2}{m_p c^2} \right) \frac{\exp-(r/r_\ell)}{r} \right\}^{1/2}, \quad (3.2)$$

which approximates to (3.1) for a weak field. Given that ($\gamma = 0$) at the *effective* proton Compton radius

$$r_p = \hbar / m_p c = 0.2103089 \text{ fm} \quad , \quad (3.3)$$

then upon substituting ($r = r_p$) into (3.2) we get

$$2 \left(\frac{a_Y^2}{m_p c^2} \right) \exp-(r_p / r_\ell) = r_p \quad , \quad (3.4)$$

therefore (3.2) becomes,

$$\gamma = \left\{ 1 - \left(\frac{r_p}{r} \right) \exp - \left(\frac{r - r_p}{r_\ell} \right) \right\}^{1/2}. \quad (3.5)$$

Now in *general*, coordinate potential V_c should be related to the metric tensor component through an expression of the form (3.1):

$$\gamma = \left\{ 1 + \frac{a_Y V_c}{m_p c^2} \right\}, \quad (3.6)$$

therefore (3.5) yields potential energy:

$$a_Y V_c = (m_p c^2)(\gamma - 1) = (m_p c^2) \left[\left\{ 1 - \left(\frac{r_p}{r} \right) \exp - \left(\frac{r - r_p}{r_\ell} \right) \right\}^{1/2} - 1 \right]. \quad (3.7)$$

This V_c is the natural potential as would be measured by a theoretical non-perturbing infinitesimal test particle. The proton hadronic charge a_Y may be derived from (3.4):

$$a_Y^2 \approx \left(\frac{m_p c^2 r_p}{2} \right) \exp \left(\frac{r_p}{r_\ell} \right) \approx 76.570171 e^2. \quad (3.8)$$

The hadronic interaction for nucleons is therefore around 76.6 times stronger than the electromagnetic interaction; and the nucleonic coupling constant α_Y is definable as:

$$\alpha_Y = \frac{a_Y^2}{\hbar c} \approx 76.6 \left(\frac{1}{137} \right) \approx \frac{5}{9} \approx \frac{1}{\sqrt{3}}. \quad (3.9)$$

As for the electromagnetic and gravitational forces, the energy-momentum tensor components for a conserved spherically-symmetric radial field are given by:

$$8\pi \left(\frac{Y}{c^4} \right) T_1^1 = 8\pi \left(\frac{Y}{c^4} \right) T_4^4 = \frac{1}{r^2} \frac{d}{dr} \left[r(1 - \gamma^2) \right], \quad (3.10)$$

$$8\pi \left(\frac{Y}{c^4} \right) T_2^2 = 8\pi \left(\frac{Y}{c^4} \right) T_3^3 = \frac{-1}{2r^2} \frac{d}{dr} \left[r^2 \frac{d}{dr} (\gamma^2) \right], \quad (3.11)$$

(see Paper I, and Wayte 1983), where Y is the NN hadronic constant, [$Y = 137e^2/m_p^2 = r_p c^2/m_p$]. This expression for momentum/stress density T_2^2 is the relativistic form of Poisson's Equation, so from substituting (3.2) in (3.11) we have:

$$8\pi \left(\frac{Y}{c^4} \right) T_2^2 = \left[\frac{(a_Y^2 / m_p c^2)}{r_\ell^2} \right] \times \left(\frac{1}{r} \right) \exp - \left(\frac{r}{r_\ell} \right). \quad (3.12)$$

Similarly, the energy density T_4^4 is given by:

$$8\pi\left(\frac{Y}{c^4}\right)T_4^4 = \left[\frac{(a_Y^2/m_p c^2)}{r_\ell}\right] \times \left(\frac{-2}{r^2}\right) \exp\left(-\frac{r}{r_\ell}\right) . \quad (3.13)$$

Integration of T_4^4 over all elemental shells from r_p to infinity yields the total hadronic field energy (W) as follows:

$$2\left(\frac{Y}{c^4}\right) \int_{r_p}^{\infty} T_4^4 4\pi r^2 dr = \left[2\left(\frac{a_Y^2}{m_p c^2}\right) \exp\left(-\frac{r}{r_\ell}\right) \right]_{r_p}^{\infty} = -r_p , \quad (3.14)$$

then by substituting ($r_p = Ym_p/c^2$),

$$W = \int_{r_p}^{\infty} T_4^4 4\pi r^2 dr = -\left(\frac{1}{2}\right)m_p c^2 . \quad (3.15)$$

Here, the negative sign indicates an attractive field constituting exactly one half of the proton mass. Analogous to the electron, half the proton mass resides in a core which carries the field. This proton core material is actually located in a torus, rotating at velocity c at mean radius r_p ; which gives the proton its spin [$1/2\hbar = (m_p/2)cr_p$]. The hadronic field charge-quanta propagate radially out and back and do not contribute to the proton spin.

Regarding this field, it is believed that each field charge-quantum actually has equivalent mass m' which is a fraction of a proton-pearl mass, (say $m'/137^2$). A smooth copious field of 'bia-pearls' is thereby produced; (bia \equiv force). All the previous analysis remains valid if a reduced Planck constant (\hbar') is assumed to go with the mass m' such that the field range is unchanged ($r_\ell = \hbar'/m'c$). This interpretation differs from the concept of a single pion exchange particle in QCD theory.

From (3.10), (3.12) and (3.13) the lateral stress T_2^2 relative to radial stress T_1^1 in the field is given by:

$$T_2^2 / T_1^1 = -r / 2r_\ell , \quad (3.16)$$

unlike the electromagnetic field in which the quanta have unitary helicity. It indicates that the field bia-pearls propagate radially at the velocity of light (since $T_1^1 = T_4^4$) but spin at a lower velocity when ($r < 2r_\ell$). At larger radii, velocities greater than c are theoretically

permissible for mechanisms inside particles. A bia-pearl therefore takes the form of a vortex, which decreases in energy with radius.

4. Hard core repulsion

Hard core repulsion exists between nucleons but not between a nucleon and anti-nucleon; see Klempt et al. (2002). This agrees with the electromagnetic force in which electrons repel each other but attract positrons. The difference between electrons and positrons is helicity; therefore hard-core repulsion could involve modification of the regular helicity of bia-pearls due to the spinning proton stirring the field at a frequency ($m_p/m_\ell = 9$) times the pearl Compton frequency. Gluonic charge g operating around the spin-loop may also be involved, as described in (8.10). Furthermore, the short-range of repulsion could satisfy (2.2), for r_ℓ replaced by r_p . These three effects can be added into (3.5) thus:

$$\gamma_{\text{NQ}} = \left\{ 1 - \left[1 - \left(\frac{m_p}{m_\ell} \frac{g}{a_Y} \right) \left(\frac{a_Y^2}{m_p c^2 r} \right) \exp - \left(\frac{r - r_p}{r_p} \right) \right] \times \left(\frac{r_p}{r} \right) \exp - \left(\frac{r - r_p}{r_\ell} \right) \right\}^{1/2} . \quad (4.1)$$

At very short range ($r \approx r_p$), it approximates to a satisfactory form:

$$\gamma_{\text{NQ}} \approx \left\{ 1 - \left(\frac{r_p}{r} \right) + 7 \left(\frac{r_p}{r} \right)^2 \right\}^{1/2} \rightarrow \{7\}^{1/2} , \quad (4.2)$$

and the proton natural quiescent potential is given by:

$$a_Y V_{\text{NQ}} = (m_p c^2) (\gamma_{\text{NQ}} - 1) . \quad (4.3)$$

Now, the expression (4.1) needs to be adjusted to take into account the finite size of a *colliding* proton such that the closest approach distance is actually $2r_p$ in contrast to the above r_p for the *infinitesimal* theoretical test particle. Then, (4.1) will become a *coupling* metric tensor component which will reduce to (4.2) at ($r = 2r_p$):

$$\gamma_{\text{COUPLING}} = \left\{ 1 - \left[1 - \left(9 \frac{g \alpha_Y}{a_Y} \right) \left(\frac{r_p}{r - r_p} \right) \exp - \left(\frac{r - 2r_p}{r_p} \right) \right] \times \left(\frac{r_p}{r - r_p} \right) \exp - \left(\frac{r - 2r_p}{r_\ell} \right) \right\}^{1/2} . \quad (4.4)$$

The *coupling* potential is now given by:

$$a_Y V_{\text{COUPLING}} = (m_p c^2) (\gamma_{\text{COUPLING}} - 1) . \quad (4.5)$$

Given this, the real *interaction* potential between the sizeable nebulous charges is found by squaring and scaling:

$$\begin{aligned} a_Y V_{\text{INTERACTION}} &= (a_Y V_{\text{COUPLING}})^2 \times (2\pi / \alpha_Y) / (m_p c^2) \\ &= (2\pi r_p) \times (V_{\text{COUPLING}})^2 \end{aligned} \quad (4.6)$$

This is plotted in Figure 1, and it fits the attractive part of the 1S_0 component given by Stoks et al. (1994) illustrated in Figure 2. Their softer repulsive core component can be matched by adding a relativistic correction, as follows.

In a head-on collision of two protons, the incident kinetic energy is converted to mass energy by the hard core repulsion until they come to rest momentarily. This relativistic increase in mass causes the protons to shrink in radius, making their cores appear softer. All radii in (4.4) are relative to r_p , therefore the effect of this shrinkage is to replace r by a foreshortened value r' given by:

$$r' = r \times \left(\frac{m_p c^2}{m_p c^2 + a_Y V_{\text{INTERACTION}}} \right), \quad (4.7)$$

as demonstrated in Figure 1, agreeing well with Figure 2. The derivation of our potential was guided by such published profiles.

The hard core field modulation may also affect the *attraction* between a nucleon and anti-nucleon. By changing (α_Y) to $(-\alpha_Y)$ in equations (4.4)(4.6), the repulsion becomes enhanced attraction, as shown in Figure 1.

We can interpret (4.6) in terms of work done when colliding nucleons which retain their charge nebulosity while their fields come together. Given $[Y = a_Y^2 / (m_p^2 \alpha_Y)]$, then equation (3.12) with (2.2) show that T_2^2 is proportional to charge density and potential. Therefore charge within a nominal volume is proportional to potential, and the form of (4.6) reminds us of the work done charging a capacitor C to voltage V by adding charge q :

$$W = \int v dq = C \int_0^V v dv = \frac{1}{2} CV^2, \quad (4.8a)$$

so we may derive an *equivalent* capacitance of the proton:

$$C = 2 \times 2\pi r_p = 4\pi r_p. \quad (4.8b)$$

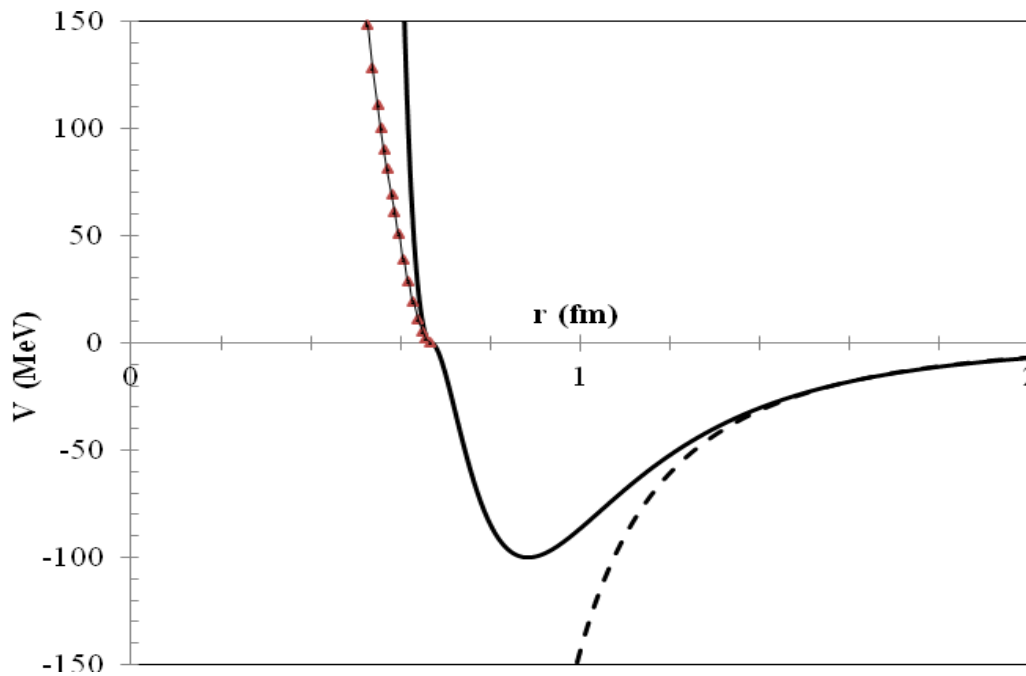


Fig.1. Nucleon interaction potential. Bold-line: potential Eq.(4.6). Triangles: relativistic correction. Dashed-line: enhanced attraction between a nucleon and anti-nucleon.

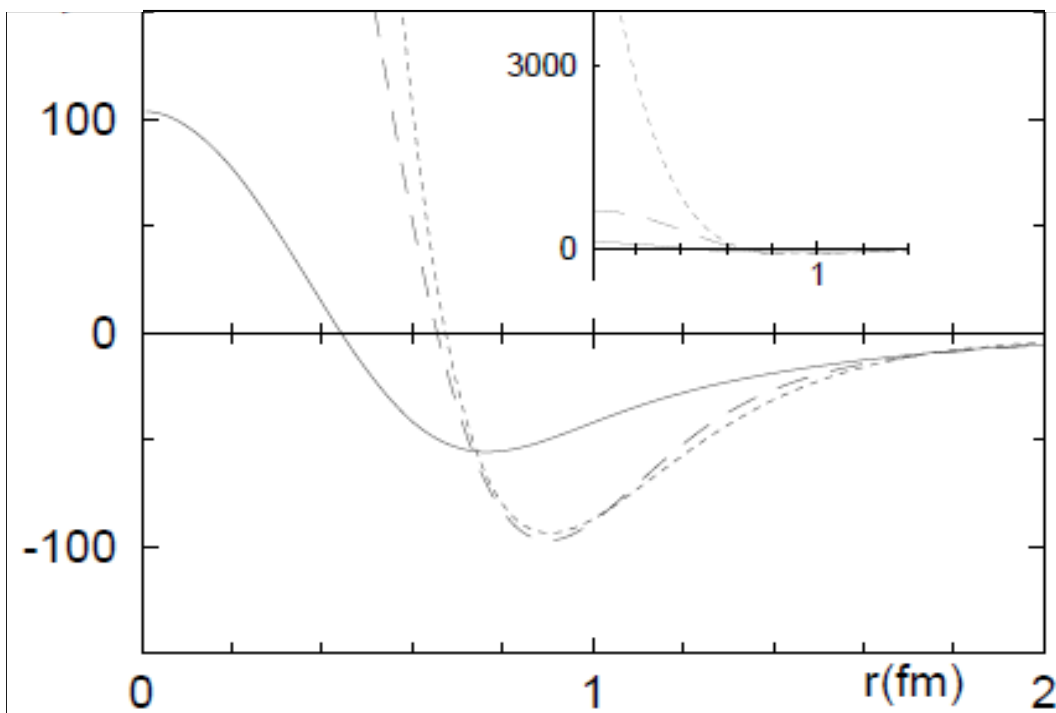


Fig.2. Copied from Stoks et al. (1994). New potentials in the np singlet.
Solid line, Nijm I; dashed line, Nijm II; dotted line, Reid93.

Thus, the equivalent capacitor is a sphere of radius $4\pi r_p$ with capacitance

$$C = 4\pi\epsilon_0 \times 4\pi r_p = 2.9 \times 10^{-25} \text{ Farads} . \quad (4.9)$$

This radius is equal to double the Compton wavelength of a proton. For this interpretation of (4.6) over the whole range including the repulsive core, only the *attractive* field of (3.12) has just been referenced, indicating that the interaction work involves an *equivalent* charge density of the nebulosity.

Although a spherically symmetric field has been assumed so far, the proton produces a toroidal near-field which approximates to a spherical field at larger radius. This will affect high energy NN collision results, especially with regard to spin polarisation.

5. Proton magnetic moment

Previous papers on the electron and muon showed how the magnetic moment analysis could involve all the component parts of those particles, from spin-loop through to fundamental elements. Likewise here, the measured proton magnetic moment exhibits features which can be directly attributed to substructure components, in common with the electron. Electromagnetic strength factors, 137, 37.7, 24 and 50 are identified in the component parts, in terms of simple geometry.

In this model, a proton is to consist of 9 pieces of approximate muonic mass arranged in two ranks of 3 parts (see Figure 3). The larger rank is the spin-loop of spin $\frac{1}{2}\hbar$, and is equivalent to the 3 quarks of QCD theory; but since they are very different from quarks they will be called trineons. These parts have equal mass and travel around a Lagrange system (see Montgomery, 2001), which is known to be a system of minimum action. Probably, the 3 parts in a rank differ in phase by $2\pi/3$, and this could be responsible for the so-called quark colour phenomenon. A trineon is complex, consisting of 3 complex pearls (analogous to gluons in QCD theory), each part consisting of 37 grains, which consist of 137 mites, which contain 50 elements each. We shall see in Section 7 that the proton creation is most easily understood if it happens via seed growth, starting with the spin-loop and working downwards to smaller elements, which can only be created in situ as space becomes available. As for the electron model, the grains, mites, and elements are treated like particles, but they are actually the individual turns of a helix around the periphery of the next larger particle.

Given that the proton spin is $\frac{1}{2}\hbar$, then the expected magnetic moment of the spin-loop would be one nuclear magneton:

$$\mu_s = \text{current} \times \text{area} = \left(\frac{e}{2\pi r_p / c} \right) (\pi r_p^2) = \frac{e\hbar}{2m_p} = \mu_N . \quad (5.1)$$

The measured value is almost 3 times this:

$$\mu_p = \mu_N \times 2.792\,847\,344\,63(84) \quad (5.2)$$

Our proton model will produce a concise expression for μ_p as:

$$\mu_p / \mu_s = 2.792\,847\,343\,12(4) = 3 \left\{ 1 + [(2\pi\alpha^{-1}) + 1]^{-1} \right\} \times \left\{ 1 - 3 \left(\pi^3 \alpha / 4e_n \right) \left[1 + (3\varepsilon) \left\{ 1 - (\delta/2) \left[1 - (\pi\alpha/2) \left\{ 1 + \mu(\pi/e_n)^2 \right\} \right] \right\} \right] \right\} . \quad (5.3)$$

Here the fine structure constant has been taken as the empirical value:

$$\alpha^{-1} = 137.035999084(21) \approx 137, \quad (5.4a)$$

while the other constants have the same values as for the electron, but different positions:

$$\delta^{-1} = 12\pi \approx 37.7, \quad \varepsilon^{-1} = 24, \quad \mu^{-1} = 16\pi \approx 50, \quad (5.4b)$$

and $e_n \approx 2.718281828459$ is the natural logarithm base.

Analysis of the magnetic moment equation (5.3) will involve some properties already seen in electron and muon structures, plus new features. The first factor 3 implies that each trineon behaves as if it has unit charge e^+ when interacting with an applied external magnetic field, even though the exterior charge of the proton is e^+ . Subsequent terms cover magnetic moments of 3 pearls per trineon, with their constituent grains, mites and elements, which are all physically much smaller particles.

The first curly bracket of (5.3) is identical to that in the electron model, and serves to include the self-interaction electromagnetic energy around the proton spin-loop, which increases the effective circulating charge. This energy is nominally $(e^2/2\pi r_p)$ but it has to be supplied by the proton itself, so it is reduced slightly to:

$$\Delta E = \left(\frac{e^2}{2\pi r_p} \right) \left[\frac{(m_p c^2 - \Delta E)}{m_p c^2} \right], \quad (5.5a)$$

which gives the required normalized value:

$$\Delta E / m_p c^2 = [(2\pi\alpha^{-1}) + 1]^{-1} . \quad (5.5b)$$

Each part of the second curly bracket in (5.3) may be explained by expanding terms:

$$1 - \left(\frac{(3) 137 (\pi / e_n)}{[137 (2 / \pi)]^2} \right) \left[1 + \left(\frac{(3) 24}{24^2} \right) \left\{ 1 - \left(\frac{37.7}{2 \times 37.7^2} \right) \left[1 - \left(\frac{(2 / \pi) 137}{[137 (2 / \pi)]^2} \right) \left\{ 1 + \frac{(2 / \pi) (\pi / 2) (\pi / e_n)^2 50}{50^2} \right\} \right] \right\} \right] \quad (5.6)$$

3 trineons 3 pearls 37 grains 137 mites 50 elements .

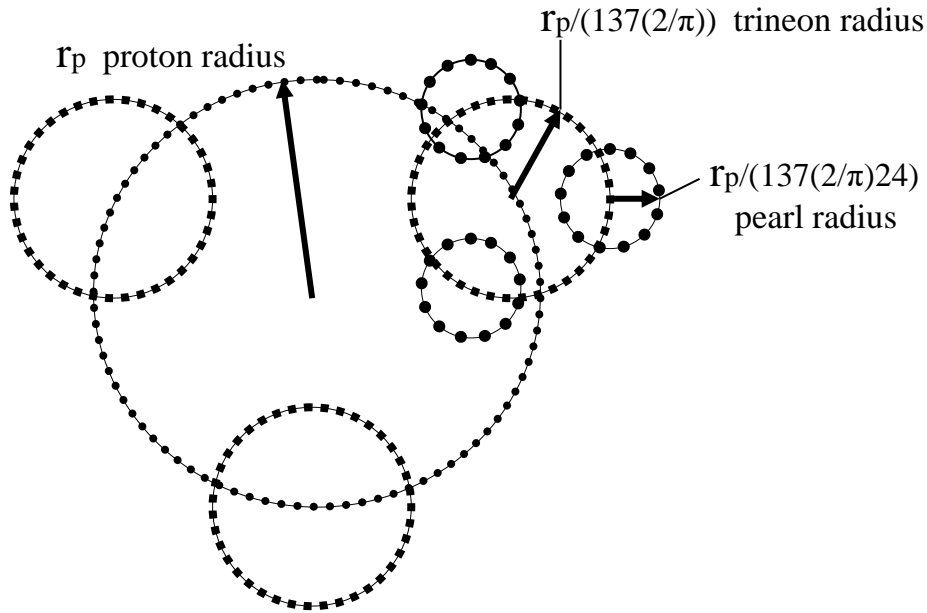


Figure 3. Schematic diagram of a proton which consists of 2 ranks incorporating 3 trineons and 3 pearls. A pearl has approximately the mass of a muon.

For clarity, the approximate forms of α , δ , ϵ , μ have been used, and the particles being described are noted underneath. In the following explanation of each term, the ‘current x area’ definition (5.1) is consistently applied with regard to current flow and particle areas.

The first round bracket in (5.6) represents the contribution to the magnetic moment from 3 trineons, running as cycloids, anti-parallel to the spin-loop, see Figure 3. A trineon is $137(2/\pi)$ times smaller than the spin-loop, so the denominator expresses the corresponding relative area. It spins with enhanced velocity [$c' = c(\pi/2)$]. The numerator factor 137 represents current flow around the 137 gluonic loops which constitute a trineon itself, (formed into 3 pearl-clumps). Factor (π/e_n) is a weighting term for these gluons.

The second round bracket represents the contribution from the 3 pearls, running as cycloids, around and parallel to their trineons, see Figure 3. A pearl is 24 times smaller than a trineon so the denominator expresses relative area. It spins with velocity c' . The numerator factor 24 is interpreted as current flow around the 24 gluonic loops which constitute the pearl itself, (braided into a peripheral helix of grains).

The third round bracket represents contribution from the 37 grains running helically, (probably left-handed), around each pearl circumference. A grain spins at velocity c' , and is 37.7 times smaller than a pearl so the denominator expresses relative area. Attenuation factor $(1/2)$ may be due to the helical propagation around the cycloidal pearl.

The fourth round bracket represents the contribution from current flow around 137 mites running helically around each grain circumference. A mite spins at velocity c' , and is $137(2/\pi)$ times smaller than a grain, so the denominator expresses relative area. The attenuation coefficient $(2/\pi)$ applies to mites and their constituent elements because of their changes in orientation as they run around a grain. Mite areas, projected parallel to the spin-loop, are thus reduced by the factor $(2/\pi)$ on average.

Finally, the last bracket represents the contribution from 50 elements running helically around each mite circumference. An element spins at velocity c , and is 50 times smaller than a mite so the denominator expresses relative area. The additional attenuation coefficient $(2/\pi)$ applies to elements because of their changes in orientation as they move. Their areas, projected parallel to the spin-loop in *two* axes, are reduced to $(2/\pi)^2$ on average. The weighting factor $(\pi/2)$ is attributed to the element spin velocity being c while its propagation velocity is c' around its mite circumference; as seen for the grain/mite transition in the electron model. Coefficient $(\pi/e_n)^2$ accounts for the internal field energy associated with the elemental material.

The 50 elements per mite are the actual source of proton electromagnetic field quanta, and may have right-handed helicity like positrons. However, in experiments on electron and neutrino scattering from protons, the pearls behave as if they have left-handed helicity. Consequently, if the elements have left-handed helicity then the field quanta must peel-off with opposite hand.

6. Proton mass

Analysis of the muon (Paper 2) showed how its mass is related to the electron mass in terms of binding energy loss and magnetic coupling effects. If proton mass is related to muon mass, it can also reveal a binding energy term:

$$m_p = 8.880243364 \times m_\mu \approx 3 \times \left[3 \left(1 - \frac{1}{2 \times 37.7} \right) m_\mu \right] , \quad (6.1)$$

where ($m_p = 1836.15267343(11) m_e$) and ($m_\mu = 206.768 2830 (46) m_e$).

At first sight, this expression could imply that a proton is just a collection of 9 muons; but in fact, the structure within a proton-pearl is very different from the structure of a *free* muon. The bracket on the right could be taken to describe binding energy of 3 pearls in a *trineon*, as if the pearls remain by attraction around the trineon circumference with a binding energy of ($m_\mu c^2 / 2 \times 37.7$) per pearl.

We shall see in Section 7 that the proton core is found to consist of a single filament of matter, winding through every element in every part, in series. Then from Section 5, the proton elemental mass is given by:

$$m_{el/p} = m_p / [(3 \times 137)(3 \times 24)(37.7)(137)(50)] . \quad (6.2)$$

For comparison, the electron structure analysis in Paper 1 showed how the electron elemental mass was given by:

$$m_{el/e} = m_e / [(137)(137)(37.7)(24)(50)] . \quad (6.3)$$

The ratio of these different elemental masses is:

$$\frac{m_{el/p}}{m_{el/e}} \approx \frac{1836}{3 \times 3} \approx 204 \approx \frac{m_\mu}{m_e} . \quad (6.4)$$

7. Creation of proton component parts

Just as the electron and muon were created in several separate stages by spiralling from previously created or newly generated seeds, so the proton structure is analysable from spin-loop to its most fundamental elements. Using previous techniques and arguments from Paper 1, every step has to be compatible with other aspects of the model, and empirically sound. The above magnetic moment analysis has been the essential basis of the following theory, with frequent reference to electron structure, given in Paper 1.

7.1 Creation of a proton spin-loop

Proton design involves 3 trineons travelling cycloidally around the spin-loop at velocity c , aligned *antiparallel* to the spin-loop. For creation of the spin-loop from a small seed, the proposed *spiralling plus seed-creation* equation is to be based on the following formula:

$$\{\ln(137/e_n) - \ln[1 + \ln(137/e_n)]\} + \{\ln 137\} \approx (2\pi^2 / e_n) . \quad (7.1.1)$$

Here the first two terms will cover spiralling open of the seed by a radial factor ($137/e_n \approx 50$), while the third term indicates that the seed itself will be created with 137 material loops on its circumference. After spiralling open from the seed radius ($r_{ps} \approx r_p / 50$), this material separates into 3 trineons, (of 137 gluonic loops each). Given the spin-loop radius [$r_p = 137(e^2/m_p c^2) = 137r_{po}$] and circumference ($'O_p = 2\pi r_p = z_p$), then (7.1.1) may be reduced to an action equation:

$$\left\{ \int_{'O_{ps}}^{'O_p} \frac{e^2}{z} \left[1 - \frac{v_z}{c} \right] \left[\frac{v_z}{c} \right] dt \right\} + \left\{ \int_{'O_{ps}/137}^{'O_{ps}} \frac{e^2}{z_h} \frac{dz_h}{c} \right\} \approx \left(\frac{\pi}{e_n} \right) \int_0^{2\pi} (m_p c r_{po}) d\theta . \quad (7.1.2)$$

The spiralling term on the left describes how a proton circumference ($'O_p$) is formed by spiralling from the spin-loop-seed circumference ($'O_{ps} = 'O_p / (137/e_n)$). It confirms that a proton behaves as if it has charge e^+ throughout the process. In the second term, the circumference of the original seed ($'O_{ps}$) consists of 137 material loops wound in a helix of radius ($'O_{ps} / 2\pi 137$), and created just before spiralling begins. These loops develop after the spiralling process into the 3 trineons. On the right, the action integral employs the original mass m_p in the spin-loop before any external hadronic field has formed, (which would reduce m_p to $m_p / 2$). The kinetic energy action is given using the classical proton radius ($r_{po} = e^2/m_p c^2$), analogous to the classical electron radius ($r_o = e^2/mc^2$) used in Paper 1. Weighting coefficient (π/e_n) accounts for internal field energy associated with the material energy.

7.2 Creation of a trineon.

Trineon design consists ultimately of a circumference of 3 complex pearls aligned *anti-parallel* to their trineon. A trineon has a radius r_o' which is $137(2/\pi)$ times smaller than the spin-loop r_p , and it rotates at a velocity $c' = c(\pi/2)$. The proposed spiralling plus seed-creation equation is to be based upon a formula somewhat like that for spin-loop creation:

$$\{\ln(24/e_n) - \ln(1 + \ln(24/e_n))\} + \{\ln 24\} \approx (\pi^3 / e_n^2) \quad . \quad (7.2.1)$$

Given the classical proton radius expression ($r_{po} = e^2/m_p c^2$), then development of (7.2.1) in the usual way yields an action integral for each of the 137 loops produced above, prior to their condensing into 3 separate trineons:

$$\left\{ \int_{O_{0s}}^{O_0} \frac{(e/137)^2}{z} \left[1 - \frac{v_z}{c'} \right] \left[\frac{v_z}{c'} \right] dt \right\} + \left\{ \int_{O_{0s/24}}^{O_{0s}} \frac{(e/137)^2}{z_h} dt \right\} \approx \left(\frac{\pi}{e_n} \right)^2 \int_0^{2\pi} \left(\frac{m_p c r_{po}}{137^2} \right) \frac{d\theta}{e_n} \quad . \quad (7.2.2)$$

The first term shows a trineon circumference ($O_0 = z_p / 137(2/\pi)$), being formed by spiralling from the trineon-seed circumference ($O_{0s} = O_0 / (24/e_n)$). In the second term, this original seed circumference has 24 material loops, in a helix of radius ($O_{0s} / 2\pi 24$), created just before the spiralling begins. These original 24 material loops grow and finally condense into 3 pearls (of 24 gluonic loops each) propagating around the trineon circumference at velocity c' while spinning at c' also. On the right side, the proton kinetic energy action is given, using classical r_{po} again. Weighting coefficient (π/e_n) accounts for field energy associated with the material energy. Factor $(1/e_n)$ indicates that a second harmonic guidewave is in control.

7.3 Creation of a pearl.

A pearl periphery O_1 consists ultimately of 37 grains which propagate helically around the circumference at velocity $c' = c(\pi/2)$, while spinning at c' . The pearl spiralling plus seed-creation equation is based upon a formula with some similarity to that for trineon creation:

$$\{\ln 37.7 - \ln(1 + \ln 37.7)\} + \{\ln 37.7\} \approx (\pi^3 / 2e_n) \quad . \quad (7.3.1)$$

Development of this in the usual way yields an action integral for each of the 24 loops produced above, prior to their condensing into 3 separate pearls:

$$\left\{ \int_{'O_{1s}}^{'O_1} \frac{(e\alpha\varepsilon)^2}{\ell} \left[1 - \frac{v_\ell}{c'} \right] \left[\frac{v_\ell}{c'} \right] dt \right\} + \left\{ \int_{'O_{1s}/37.7}^{'O_{1s}} \frac{(e\alpha\varepsilon)^2}{\ell_h} dt \right\} \approx \left(\frac{\pi}{e_n} \right) \int_0^{2\pi} \left(\frac{m_p c r_{po}}{2(137 \times 24)^2} \right) d\theta. \quad (7.3.2)$$

The first term covers spiralling growth of the pearl by factor 37.7 from a seed of circumference ($'O_{1s} = 'O_1 / 37.7$). Final pearl circumference is 24 times less than the trineon, ($'O_1 = 'O_0 / 24$). In the second term, the original pearl-seed circumference ($'O_{1s}$) has 37.7 material loops in a helix of radius ($'O_{1s} / 2\pi 37.7$), created just before spiralling begins. These 37.7 loops grow into the grainy helix, propagating around the pearl circumference at velocity c' while spinning at c' . On the right side, weighting coefficient (π/e_n) accounts for field energy associated with the material energy.

7.4 Creation of a grain.

A grain periphery $'O_2$ consists of 137 mites which travel around the grain at velocity c' while spinning at velocity c' also. The grain spiralling plus seed-creation equation is based on a formula like that for spin-loop creation:

$$\{ \ln(137/e_n) - \ln(1 + \ln(137/e_n)) \} + \{ \ln(137) \} \approx (2\pi^2 / e_n). \quad (7.4.1)$$

This may be developed into an action integral:

$$\left\{ \int_{'O_{2s}}^{'O_2} \frac{(e\alpha\varepsilon\delta)^2}{\xi} \left[1 - \frac{v_\xi}{c'} \right] \left[\frac{v_\xi}{c'} \right] dt \right\} + \left\{ \int_{'O_{2s}/137}^{'O_{2s}} \frac{(e\alpha\varepsilon\delta)^2}{\xi_h} dt \right\} \approx \int_0^{2\pi} \frac{m_p c r_{po}}{(137 \times 24 \times 37.7)^2} \left(\frac{2}{e_n} \right) d\theta. \quad (7.4.2)$$

The first term covers spiralling growth of the grain by a factor $(137/e_n)$ from a seed circumference [$'O_{2s} = 'O_2 / (137/e_n)$]. Final grain circumference is 37.7 times less than the pearl, ($'O_2 = 'O_1 / 37.7$). In the second term, the original grain-seed circumference ($'O_{2s}$) has 137 material loops, in a helix of radius ($'O_{2s} / 2\pi 137$), created just prior to spiralling. These grow in the grain final circumference into 137 mites (each of circumference, $'O_3 = 'O_2 / 137(2/\pi)$) which propagate and spin at velocity c' . On the right-side, factor 2 is for weighting, and $(1/e_n)$ indicates a second harmonic guidewave in operation here.

7.5 Creation of a mite.

A mite periphery contains ($16\pi \sim 50$) elements, which travel around the circumference at velocity c' while spinning at c . The mite spiralling plus seed-creation equation is based upon a formula like that for grain creation:

$$\{\ln 50 - \ln(1 + \ln 50)\} + (\pi/2)\ln 50 \approx (2\pi^3 / e_n^2). \quad (7.5.1)$$

Development of this in the usual way shows how a mite-seed evolves by spiralling open, according to this action integral:

$$\left\{ \int_{O_{3S}}^{O_3} \frac{(e\alpha\varepsilon\delta\alpha)^2}{\rho} \left[1 - \frac{v_\rho}{c'} \right] \left[\frac{v_\rho}{c'} \right] dt \right\} + \left\{ \int_{O_{3S}/50}^{O_{3S}} \frac{(e\alpha\varepsilon\delta\alpha)^2}{\rho_h} dt \right\} \approx \left(\frac{\pi}{e_n} \right)^{2\pi} \int_0^{2\pi} \frac{m_p c r_{po}}{(137 \times 24 \times 37.7 \times 137)^2} \left(\frac{2}{e_n} \right) d\theta \quad (7.5.2)$$

The first integral covers spiralling action for the mite increasing from a seed circumference O_{3S} to its final circumference ($O_3 = 50 \times O_{3S}$), which is $137(2/\pi)$ times less than the grain, ($O_3 = O_2/(137(2/\pi))$). The second integral represents scalar potential action of creating 50 elemental loops, which travel around the mite-seed circumference at velocity c' while spinning at c , prior to the mite spiralling process. On the right side, m_p is used rather than $m_p/2$ because this process applies prior to an external field forming. Weighting coefficient (π/e_n) accounts for internal field energy associated with the element material energy. Factor $(2/e_n)$ indicates a second harmonic guidewave is in operation here, with 2 times weighting.

A final mite circumference O_3 then consists of a helix of 50 material elements travelling at c' around the circumference, while spinning at velocity c according to the formula:

$$\ln 50 \approx (\pi^2 / e_n), \quad (7.5.3)$$

which may represent an action integral:

$$\int_{O_3/50}^{O_3} \frac{(e\alpha\varepsilon\delta\alpha)^2}{\rho_h} dt \approx \left(\frac{\pi}{e_n} \right)^{2\pi} \int_0^{2\pi} \frac{m_p c r_{po}}{2(137 \times 24 \times 37.7 \times 137)^2} d\theta \quad (7.5.4)$$

Weighting coefficient (π/e_n) appears in the magnetic moment analysis (5.6), and accounts for the field energy associated with the material energy. These 50 material elements in each mite are fundamental, and emit tethered electromagnetic field quanta with right-handed helicity.

8. Gluons.

Experimental evidence can be interpreted in QCD such that 3 quarks in the proton are bound together by the strong force due to gluons carrying charged colour force quanta. Herein, we will interpret gluons as the 9 pearls constituting 3 trineons, carrying charge quanta to confine the trineons to the toroidal spin-loop. The exterior nuclear field charge, covered in Sections 2-4 is also carried by the pearls/gluons and is similar in substance to the internal colour charge.

Our model of charmonium (Wayte, Paper 3) has employed the logarithmic potential to explain the gluon colour field between a quark and anti-quark, see Quigg and Rosner (1979, pp217-223) For charmonium fundamental mass M_C and characteristic dimension r_q , the potential energy was found to be given by:

$$V(r) \approx \frac{M_C c^2}{2 \times 2^{1/2}} \ln \left(\frac{r}{r_q} \right) . \quad (8.1)$$

For the proton here, this potential energy will be modified thus:

$$V(r) = \frac{m_p c^2}{2} \ln \left(\frac{r}{r_p} \right) , \quad (8.2)$$

where the proton radius is $[r_p = 137(e^2/m_p c^2) = \hbar/m_p c]$. At equilibrium ($r = r_p$) the effective potential is zero, but the *field* is operating to confine the trineons against electromagnetic repulsion and centrifugal force, and to resist disintegration in collisions. Then the metric tensor component (γ) for Einstein's equations will take the form:

$$\gamma = \left[1 + \frac{V(r)}{m_p c^2} \right] = \left[1 + \frac{1}{2} \ln \left(\frac{r}{r_p} \right) \right] , \quad (8.3)$$

which would be zero for trineons travelling in a minimum loop of radius $[r_{ot} = r_p \exp(-2)]$. Potential (8.2) will be applied to a flux-tube of colour charge linking the trineons around the proton spin-loop.

There is a solution of Einstein's Equations for a conserved linear field, which could apply to a toroidal flux-tube. Let x represent distance around the flux-tube, of cross-sectional area $4\pi r_{ot}^2$, with internal colour field carried by the pearl/gluons

constituting trineons. Components of the energy-momentum tensor are derived from Dingle's formulae (Tolman, 1934, p. 253), for the line element:

$$ds^2 = -\gamma^{-2}dx^2 - dy^2 - dz^2 + \gamma^2 dt^2 \quad . \quad (8.4)$$

These components are mathematically:

$$8\pi\left(\frac{S'}{c^4}\right)T_1^1 = 8\pi\left(\frac{S'}{c^4}\right)T_4^4 = 0 \quad (8.5a)$$

$$8\pi\left(\frac{S'}{c^4}\right)T_2^2 = 8\pi\left(\frac{S'}{c^4}\right)T_3^3 = -\frac{1}{2}\frac{d^2\gamma^2}{dx^2} = -\gamma\frac{d^2\gamma}{dx^2} - \left(\frac{d\gamma}{dx}\right)^2 \quad . \quad (8.5b)$$

Then, upon introducing γ from (8.3) and working with radius r for convenience, we get the colour field tangential momentum/stress density, which appears to consist of two parts for the charge particles and their quanta:

$$8\pi\left(\frac{S}{c^4}\right)T_2^2 = \left|\frac{\gamma}{2r^2}\right| - \left|\frac{1}{2r}\right|^2 \quad . \quad (8.6a)$$

Given this, the apparently-zero longitudinal momentum density T_1^1 in (8.5a) must refer to gluons travelling in opposite directions around the spin-loop. It can be applied to real unidirectional trineons by changing the form thus:

$$8\pi\left(\frac{S}{c^4}\right)T_1^1 = 8\pi\left(\frac{S}{c^4}\right)T_4^4 \Rightarrow \left|\frac{-1}{2r}\right|^2 + \left|\frac{1}{2r}\right|^2 \quad . \quad (8.6b)$$

Integration of this T_4^4 from ($r = r_{ot}$) to ($r = \infty$), will yield the total colour field energy.

First,

$$2\left(\frac{S}{c^4}\right)\int_{r_{ot}}^{\infty}T_4^4(4\pi r_{ot}^2)dr \Rightarrow \left|\frac{-r_{ot}}{4}\right| + \left|\frac{r_{ot}}{4}\right| \quad , \quad (8.7)$$

then upon setting [$r_{ot} = Sm_p/c^2$], analogous to [$r_p = Ym_p/c^2$] in (3.14), the colour field energy amounts to 25% of the proton mass energy:

$$W = -\int_{r_{ot}}^{\infty}T_4^4(4\pi r_{ot}^2)dr = \frac{1}{4}m_p c^2 \quad . \quad (8.8)$$

This colour field is wrapped around the proton spin-loop multiple times from minimum ($2\pi r_{ot}$) to effective infinity. Since half the proton's energy is already in its external field, see (3.15), then only a quarter now remains for the pearl/gluon bodies.

The tangential momentum density T_2^2 may be integrated to get a similar result:

$$2\left(\frac{\mathbf{S}}{c^4}\right)\int_{r_{ot}}^{\infty}T_2^2(4\pi r_{ot}^2)dr = \left|\frac{-r_{ot}}{4}\right| + \left|\frac{r_{ot}}{4}\right|. \quad (8.9)$$

This means that the colour field has unitary helicity on average and propagates at the velocity of light. The two equal parts, on the right hand sides of (8.7) and (8.9), implies that each colour charge particle has half its energy in a core and half in its quantum field, like an electron.

Our proton model has been used to help interpret the running of the strong coupling constant with momentum transfer in a collision process, see Wayte, (Paper 4). This running is found to involve pearl mass (m_ℓ) rather than the proton mass, in a monotonic law. The strong coupling constant derived therein ($\alpha_s = 1.0406845$) describes the gluon coupling which binds the proton's core components together. This can be related to the exterior nuclear force constant ($\alpha_Y = 0.55876$) of (3.9) which binds nuclei together. Given that the strong and nuclear forces are made of the same material, they should be linked:

$$\alpha_s = \frac{g^2}{\hbar c} \approx \left(\frac{e_n}{2}\right)^2 \alpha_Y \approx \left(\frac{e_n}{2}\right)^2 \frac{a_Y^2}{\hbar c}, \quad \text{or} \quad g \approx \left(\frac{e_n}{2}\right) a_Y. \quad (8.10)$$

where ($g \approx 11.94e$) is an equivalent gluonic charge and ($e_n = 2.718282$). Coefficient (e_n) is split between charge ($g = a_Y e_n/2$) for the colour field, plus an equivalent mass for the pearl/gluon source of the field according to (8.8). Thus, given integration to infinity in (8.8), the colour field material is *effectively* wrapped around the proton spin-loop, layer upon layer to infinity. If (e_n) is expressed as a sum of components:

$$e_n = \left\{1 + (1-1/e_n)^1 + (1-1/e_n)^2 + (1-1/e_n)^3 + \dots\right\}, \quad (8.11)$$

then the total material is equivalent to the sum of layers which decrease in content one after the other by factor $(1-1/e_n)$. The material which peels-off each layer ($1/e_n$) sums exactly to charge (a_Y) constituting the exterior nuclear field/residual strong force. Hence the charge/mass ratio of the colour field is $(a_Y e_n/2)/(m_p c^2/4)$, which is (e_n) times that for the nuclear field $(a_Y)/(m_p c^2/2)$. This proposed analysis from (8.4) to (8.11) confirms conservation of charge and mass.

From (8.10), the *total* charge carried by pearl/gluons is ($a_T = a_Y + g$) so there is a strength constant (α_T) given by:

$$\alpha_T = (a_Y + g)^2 / \hbar c \approx 3\alpha_s, \quad (8.12)$$

which reminds us of 3 trineons in a proton.

Potential energy (8.2) can alternatively be written to include g^2 as:

$$V(r) = \frac{g^2}{(2\pi r_p / 3)} \ln\left(\frac{r}{r_p}\right), \quad (8.13)$$

where the denominator equals distance between trineons around the spin-loop. This expression implies ($\alpha_s \approx \pi/3$), slightly greater than the observed value or (8.10) due to small corrections involving the complex proton design.

Given (8.12) (8.13), the proton's total colour charge potential energy is proportional to its electromagnetic potential energy:

$$\frac{a_T^2}{(2\pi r_p / 3)} \approx \left(\frac{m_\ell}{m_e}\right) \times \frac{e^2}{r_p}. \quad (8.14)$$

The various constants used throughout this work are related:

$$\begin{aligned} Y &= \frac{r_p c^2}{m_p}, \quad S = \frac{r_{ot} c^2}{m_p}, \quad r_{ot} = \frac{r_p}{e_n^2}, \quad Y \approx S e_n^2, \quad Y \alpha_Y \approx 4 S \alpha_s, \\ \alpha &= \frac{e^2}{\hbar c}, \quad \alpha_Y \approx 76.6 \alpha, \quad \alpha_s \approx \alpha_Y \frac{e_n^2}{4}, \quad \alpha_T \approx 3 \alpha_s, \quad \alpha_T \approx \frac{m_\ell}{m_e} \frac{2\pi}{3} \alpha. \end{aligned} \quad (8.15)$$

9. Electromagnetic charge uniqueness.

The electron and proton have charges which are accurately equal in magnitude, but their masses and internal mechanisms are very different. Furthermore, an electron-positron pair may be produced from high energy photons without reference to a proton. So it appears to be necessary for charges to be self-contained and absolute. Fermion spin angular momentum is also absolute and may be related to charge.

First, the theoretical classical electromagnetic radius of an electron, muon or proton has the form:

$$r_o = e^2 / m_o c^2 \quad . \quad (9.1)$$

This is based on the hypothesis that work would be done in assembling incremental charges against their mutual repulsion force, as may be expressed:

$$W = \int \int \frac{q dq}{r^2} dr = \left[\frac{1}{2} \frac{q^2}{r} \right]_{r=\infty, q=0}^{r_o, q=e} = \frac{1}{2} \left(\frac{e^2}{r_o} \right) \quad . \quad (9.2)$$

Then (9.1) makes ($W = \frac{1}{2} m_o c^2$), as if the work done is stored in the particle as mass. The remaining mass energy ($\frac{1}{2} m_o c^2$) must be attributed to the original charges. Even if such a classical assembly process does not occur in reality, it is proposed that particle production conserves energy and charge, so that (9.2) and the inverse process of dispersion would be equivalent.

Second, the theoretical radius (9.1) may not always exist physically but the real spin radius is invariably given by ($r_s = 137 r_o = \hbar / m_o c$). Thus for fermions, their spin is:

$$s = (m_o / 2) c r_s = \hbar / 2 \quad , \quad (9.3)$$

and the electric charge can be defined absolutely in terms of spin by:

$$e = \pm \{2cs / 137\}^{1/2} \quad , \quad (9.4)$$

which is independent of particle mass, size, or detailed design. Then the relatively large proton mass is equivalent to work done in forcing charge into the relatively small dimensions. Obviously, everything depends on particles having spatial volume with real angular momentum rather than being theoretical singularities with abstract spin.

Calculations of magnetic moment in Section (5) and creation-action in Section (7) depended upon the charge being divisible among the various substructures; so we need a charge formula applicable to the fundamental elements in a proton. For an *electron* in Paper 1 such a formula was found which was based upon allocating 3 curls of charge Δq to each *element*. In addition, there needed to be some field material holding the 3 charge-curls in place, effectively increasing their weight to $3(\pi/e_n)$. Now the total number of elements per electron was given in Paper 1 as:

$$n_e = 137 \times 137 \times 37.7 \times 24 \times 50 = 8.5405 \times 10^8 \quad . \quad (9.5)$$

and the electron total charge was therefore:

$$e = n_e \times 3(\pi / e_n) \times \Delta q = 2.9611 \times 10^9 \Delta q \quad . \quad (9.6)$$

When all the charge-curls were situated in a single circumferential helix of cross-sectional radius r_q and unitary pitch, the overall electromagnetic action was expressed as:

$$\int_x \frac{e^2}{x} dt \approx 3 \left(\frac{\pi}{e_n} \right) \times \int_0^{2\pi} m_e c r_{oe} d\theta \quad , \quad (9.7)$$

where ($e^2/c = m_e c r_{oe}$) for the electron, and x extends from $2\pi r_q$ to $2\pi r_q \{n_e \times 3(\pi / e_n)\}$ with ($dt = dx/c$). This primeval loop of around 3×10^9 charge-curls is a most basic definition of electron *charge*.

Similarly for a *proton* of unit charge e^+ , the effective total number of elements will be taken as:

$$n_{tri} = 137 \times 24 \times 37.7 \times 137 \times 50 = 8.5405 \times 10^8 \quad . \quad (9.8)$$

The first term represents a spin-loop seed of 137 loops *before* separating into 3 trineons, as in creation equation (7.1.1). Each of these loops has a helix of 24 smaller loops according to (7.2.1), which later grow and separate into 3 pearls. Factor 37.7 represents the number of grains in each pre-pearl in equation (7.3.1). The next factor 137 is that for the mites in a grain, see (7.4.1). Finally, there are 50 elements per mite, as in (7.5.1). Clearly n_{tri} is equal to n_e during the creation stages of the proton, which suggests that the final total charge should be the same as expressed in (9.6), though it is distributed differently.

10. Creation of a Neutron

The neutrons in a neutron star are formed during the gravitational collapse of a massive star in a supernova event because of great pressure forcing free electrons onto protons. Consequently, a simple mechanical neutron model will consist of a proton orbited by a heavy-electron, in such a way as to account for the neutron's magnetic moment and its empirical mass.

10.1 Magnetic moment

It was shown in Section (5) that the proton spin-loop has radius [$r_p = 137(e^2/m_p c^2)$], and the measured magnetic moment is [$\mu_p \approx +2.792\ 847(e\hbar/2m_p)$]. Now, let there be a "heavy-electron" orbiting around a proton at chosen radius [$r_{he} = r_p(e_n\sqrt{3})$] with velocity c , which could produce a magnetic moment according to (5.1):

$$\mu_{he} = \left(\frac{-e}{2\pi r_{he}/c} \right) (\pi r_{he}^2) = -\frac{e c r_{he}}{2} = -(e_n \sqrt{3}) \times \mu_N = -4.708202 \mu_N . \quad (10.1.1)$$

Then the resultant neutron magnetic moment should be around:

$$\mu_n \approx \mu_p + \mu_{he} \approx -1.915\ 355 \mu_N , \quad (10.1.2)$$

which compares with the empirical value $\mu_n = -1.913\ 0427(5) \mu_N$.

10.2 Heavy-electron mass

Since the chosen orbit radius r_{he} is less than the radius of a *free* electron core ($r_o = e^2/m_e c^2$), it is proposed that the "heavy-electron" takes the physical form of a *heavy-electron core*. This core surrounds the proton as a thin torus of charged matter, as described in Paper 1. Work done to compress a free electron into this small core size in this location is effectively retained as the increased mass energy. Given (r_{he}) above, the heavy-electron mass might be as straightforward as:

$$m'_{he} = \left(\frac{e^2}{c^2 r_{he}} \right) = \alpha m_p \left(\frac{r_p}{r_{he}} \right) = 2.84589 m_e . \quad (10.2.1)$$

However, the neutron mass [$m_n = 1838.683\ 661\ 73(89)m_e$] is only greater than the proton mass [$m_p = 1836.152\ 673\ 43(11)$] by [$2.5309\ 883m_e$]; so we need a better description of m_{he} . Namely, let the heavy-electron mass be given approximately by the formula:

$$m_{he} c^2 = 3m_e c^2 \left\{ 1 - \frac{e^2}{3m_e c^2 (2\pi r_{he})} \right\} = 2.547 m_e c^2 \approx (m_n c^2 - m_p c^2) . \quad (10.2.2)$$

Our interpretation of this is that the heavy-electron comprises 3 parts of nominal electronic mass, which are bound together by self-interaction of its electromagnetic guidewave force around the orbit $2\pi r_{he}$, (just as a trineon consists of 3 pearls bound by gluons). Existence of the 3 component parts will be supported later by (10.2.7) and (10.3.4). This interpretation

assumes that compression work ultimately adds $(1.5309m_e c^2)$ to a free electron mass and the final heavy-electron is internally well bound and stable. The central proton does not affect this value of heavy-electron energy.

The original free electron spin-loop was compressed inwards by a factor of 137, to its seed size (r_{es} in Paper 1). This would happen in steps, rather than a single jump, because action needs to be quantised in a simple way. Possibly there would be 5 steps given by:

$$\ln 137 \approx \pi \left(1 + e^{-1} + e^{-2} + e^{-3} + e^{-4} \right) \quad . \quad (10.2.3)$$

For each step, the spin-loop material spirals-inward at azimuthal velocity c . Equation (10.2.3) may be developed into an action expression:

$$- \int_{2\pi r_e}^{2\pi r_{es}} \frac{e^2}{z} dt \approx \int_0^{2\pi} \frac{m_e}{2} c r_o \left(1 + \frac{1}{e_n} + \frac{1}{e_n^2} + \frac{1}{e_n^3} + \frac{1}{e_n^4} \right) d\theta \quad . \quad (10.2.4)$$

Here, the steps employ first to fifth harmonic guidewave frequencies, respectively. Clearly a single jump of size 137 would not accommodate velocity c , since $[\ln 137 \approx \pi(\pi/2)]$ implies velocity $[c' = c(\pi/2)]$.

The collapsing spiral has the simple form:

$$r = r_e \exp(-\phi/2\pi). \quad (10.2.5)$$

If the azimuthal material velocity is constant at c , then ($rd\phi = cdt$) and consequently, the instantaneous electron circumference is

$$2\pi r = 2\pi r_e - ct. \quad (10.2.6)$$

A controlling guidewave-loop collapses with the material, propagating at velocity c also. The total spiral rotates ($4.92 \approx \ln 137$) times and has the same shape as for electron creation, even though the velocities are different. It is necessary that this compressed electron takes the *core* design (see Section 2 of Paper 1) because miniaturising the complete electron design does not produce the correct mass.

After the electron spin-loop has been compressed down to its core radius r_o , further pressure reduces it to r_{he} . This is quantisable, in terms of action, because $\ln(r_{he}/r_o) = \ln(2.84589) \approx \pi/3$, which leads to an action integral:

$$- \int_{2\pi r_o}^{2\pi r_{he}} \frac{e^2}{z} dt \approx \int_0^{2\pi/3} \frac{m_e}{2} c r_o d\theta \quad . \quad (10.2.7)$$

Phase factor ($2\pi/3$) implies the separation of material into 3 particles during electron collapse, as allowed by (10.2.2).

Besides satisfying (10.2.2) for mass, the radius of the heavy-electron [$r_{he} = r_p(e_n\sqrt{3})$] is critical for stability because quantisation is suggested by the formula:

$$\ln(r_{he}/r_p) \approx \pi/2 \quad (10.2.8)$$

This will be interpreted such that the toroidal heavy-electron propagates spiralling circular *feeler* guidewaves inwards from its position at r_{he} to the proton spin-loop at r_p . These are reflected back so continual interaction helps keep the heavy-electron stable in position. For an equivalent guidewave charge δe^2 and mass δm_{he} , the action integral for this loop spiralling inwards and reflecting back is from (10.2.8):

$$-2 \int_{2\pi r_{he}}^{2\pi r_p} \frac{\delta e^2}{z} dt \approx \int_0^{2\pi} \frac{\delta m_{he}}{2} c r_{he} d\theta \quad , \quad (10.2.9)$$

where $(\delta e^2/c = \delta m_{he} c r_{he})$ and $(dz = c dt)$.

10.3 Neutron lifetime

Lifetime of the free neutron may be related to action around the heavy-electron in the same way as the muon lifetime was treated in Paper 2. The period of the heavy-electron is given by:

$$t_{he} = 2\pi r_{he} / c = 2.07526 \times 10^{-23} \text{ secs}, \quad (10.3.1)$$

while the measured neutron lifetime is:

$$\tau_n = 879.4 \pm 0.6 \text{ secs}. \quad (10.3.2)$$

Let $(c\tau_n)$ be equal to a number N_n of the heavy-electron circumferences (ct_{he}) ; then upon taking logarithms we get a familiar format:

$$\ln N_n = \ln(c\tau_n / ct_{he}) = 59.0095 \approx 137 \left(\pi / e_n^2 \right) \quad . \quad (10.3.3)$$

This may be developed by introducing $(e^2/c = m_{he} c r_{he})$, to give an expression for the action around the N_n heavy-electron orbits:

$$\int_{2\pi r_{he}}^{N_n(2\pi r_{he})} \frac{e^2}{z} dt \approx 137 \times \int_0^{2\pi} \frac{m_{he} c r_{he}}{2} \left(\frac{1}{e_n^2} \right) d\theta \quad . \quad (10.3.4)$$

Here, $(1/e_n^2)$ on the right implies a third harmonic guidewave, which is perfect for stabilising the 3 components of the heavy-electron. Distance $c\tau_n$ could represent a coherence length for these guidewaves.

An equivalent of (10.3.3), plus (10.2.8) is:

$$\ln N_n = \ln(c\tau_n / ct_{he}) = 59.0095 \approx 37.7(\pi/2) \approx 37.7 \ln(r_{he} / r_p) . \quad (10.3.5)$$

This with (10.2.9) may be developed to give an expression for the action around N_n heavy-electron orbits in terms of the stabilising feeler guidewaves spiralling between the proton spin-loop and the heavy electron:

$$N_n \int_{2\pi r_{he}}^{2\pi r_{he}} \frac{\delta e^2}{z} dt \approx 37.7 \times \int_{2\pi r_p}^{2\pi r_{he}} \frac{\delta e^2}{z} dt . \quad (10.3.6)$$

11. Compatibility with Standard Model

This model for a static proton has been successful at explaining the Yukawa-type potential, the reality of spin, anomalous magnetic moment, and the gluon field. On the other hand, the QCD Standard Model of particle interactions has been very successful at accounting for observations from high energy collision experiments. The conceptual differences between these two models might be explained if particles in collisions engender characteristics not apparent in static models. That is, the trineons in a proton may interact with incident particles in the same way as quarks do in QCD theory.

Consider Figure 4 wherein the proton is depicted as trineons A, B, C, travelling around the spin-loop at the velocity of light. Each trineon has a charge (+e) but only emits an electromagnetic field due to (+e/3) into the *exterior* space, so the proton's total external charge is (+e) as observed. Trineons also emit an electromagnetic field in the direction of travel *around* the spin-loop, equivalent to (+2e/3) each.

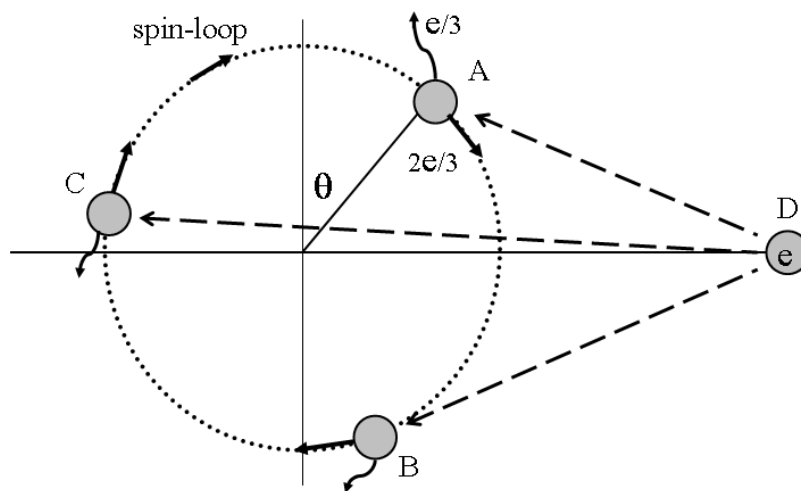


Fig.4 A schematic proton consisting of 3 trineons in the spin-loop, each with external and internal electromagnetic fields due to charge $(e/3)$ and $(2e/3)$, as experienced by an incident charged particle D.

Consequently, an energetic incident particle D (charge $+e$) could interact with an individual trineon depending upon the position and *direction* of that trineon. For example, let interaction of D on A vary as $e[e/3 + (2e/3)\cos(\theta)]$, whereas D on B will vary as $e[e/3 + (2e/3)\cos(\theta+120^\circ)]$, and D on C will vary as $e[e/3 + (2e/3)\cos(\theta+240^\circ)]$. These three interactions of particle D are shown overlaid in Figure 5. Clearly the *effective interaction charge* for each trineon can vary from (e) to $(-e/3)$. The sum for all three trineons is (e) .

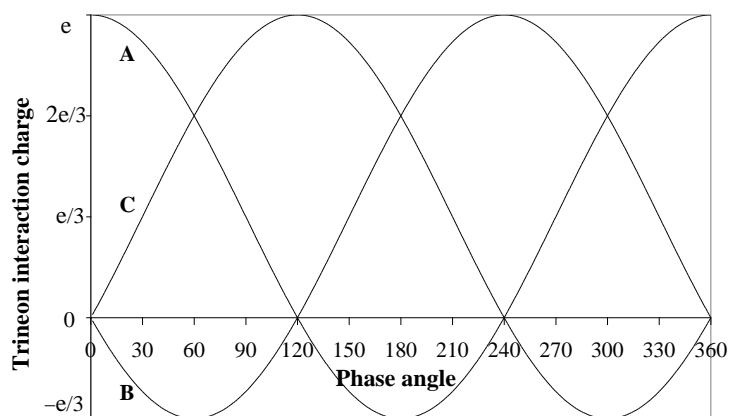


Fig.5 Variation of *interaction charge* for trineons A,B,C.

For correspondence with the Standard Model, we require the apparent effect of quarks, namely $A(+2e/3)$, $B(-e/3)$, and $C(+2e/3)$, which occur at $(\theta = 60^\circ)$ where the squared values are nearest to each other and sum to (e^2) , ie: $A(4e^2/9) + B(e^2/9) + C(4e^2/9)$. The average of $[e/3 + (2e/3)\cos(\theta)]^2$ over one spin-loop cycle, summed for 3 trineons, is also (e^2) .

Thus, the effect of a negative *interaction charge* $(-e/3)$ can happen for a collision process wherein a trineon reacts according to its *internal* mechanism and *direction* of travel. Trineons are tightly confined by strong force gluons within a proton, so any collision of an incident particle with a single trineon might appear to involve a quark of spin $(1/2)$.

For the neutron model in Section 10, a heavy-electron closely orbits the proton to counterbalance its *exterior* positive charge. In this case, interaction of D on A varies as $e[(2e/3)\cos(\theta)]$, whereas D on B will vary as $e[(2e/3)\cos(\theta+120^\circ)]$, and D on C will vary as $e[(2e/3)\cos(\theta+240^\circ)]$. Then the *effective interaction charge* for each trineon can vary from $(2e/3)$ to $(-2e/3)$. The sum for all three trineons is always zero. For correspondence with the Standard Model, we require the apparent effect of quarks such as $A(-e/3)$, $B(-e/3)$, and $C(+2e/3)$, which occurs at $(\theta = 120^\circ)$ where the squared values are nearest to each other.

12. Conclusion

A composite model of a proton has been developed which exhibits known properties. Einstein's equations of general relativity have incorporated a Yukawa-type potential in order to define a hadronic force constant $\alpha_Y \approx \alpha(137/\sqrt{3})$. Proton mass has been related to muon mass, and the magnetic moment analysis has terms very similar to those employed for the electron. The 3 main constituents, named trineons are very small and possess little spin themselves, but travel around the proton spin-loop together to generate observed proton spin $\frac{1}{2}\hbar$. Action integrals have been proposed for creating the entire substructure in separate stages, consecutively from spin-loop through to fundamental elements. Gluon energy was quantified and found to be in agreement with other work on charmonium. The gluon colour field was related to hadronic force and proton energy. The uniqueness of electronic charge has been explained in terms of a primeval loop of elementary charges, which satisfies a universal action integral. A neutron model was

proposed, consisting of a proton orbited by a heavy-electron which generates the empirical magnetic moment. Lifetime of a free neutron has been attributed to the finite coherence length of guidewaves around the heavy-electron. Finally, compatibility with the quarks of the Standard Model has been recognized for interactions between particles.

Acknowledgement

I would like to thank Imperial College Library staff and R. Simpson for typing.

References

- Bugg D V 1981 *Prog Part Nucl Phys.* **7** 47-112 ed DH Wilkinson, Oxford, Pergamon.
- Fraunfelder H and Henley E M 1991 *Subatomic Physics, 2nd Ed*, Prentice-Hall Inc. NJ.
- Iachello F 2004 *European Phys. J.* **A19** 29-34
- Klempt E, et al. 2002 *Physics Reports* **368** 119-316
- Krisch A D 1992 *Nuclear Phys.B Proc. Supp.* **25** 285-293
- Martin B R & Shaw G 1997 *Particle Physics, 2nd Ed*, J Wiley, England
- Montgomery R 2001 *Not Amer Math Soc* **48** 471-475
- Perkins D H 2000 *Introduction to High Energy Physics, 4th Ed*, Cambridge Univ. Press
- Quigg C and Rosner J L 1979 *Phys. Reports* **56** 167-235
- Sick I 2005 *Prog Particle Nuclear Phys* **55** 440-450
- Signell P 1980 *Proc Telluride Conf on the (pn) Reaction and the Nucleon-Nucleon Force*
ed CD Goodman et al, NY, Plenum 1-21
- Stoks V G J, Klomp R A M, Terheggen C P F, and de Swart J J
1994 *Phys Rev* **C49** 2950-2963; arXiv:nucl-th/9406039v1
- Wayte R 1983 The Universal Solution of Einstein's Equations of General Relativity.
Astrophys & Space Science **91** 345-380; <https://ui.adsabs.harvard.edu/>
- Wayte R (Paper 1) 2012 A Model of the Electron, vixra.org
- Wayte R (Paper 2) 2012 A Model of the Muon, vixra.org
- Wayte R (Paper 3) 2019 A Model of Charmonium (Revised), vixra.org
- Wayte R (Paper 4) 2017 Running of Electromagnetic and Strong Coupling Constants
(Rev2), vixra.org